Colloids and Surfaces B: Biointerfaces 115 (2014) 212–218

Contents lists available at ScienceDirect

Colloids and Surfaces B: Biointerfaces

journal homepage: www.elsevier.com/locate/colsurfb

Generation of nano-sized core–shell particles using a coaxial tri-capillary electrospray-template removal method

Lihua Cao [a], Jun Luo [a], Kehua Tu [a,b], Li-Qun Wang [a,b,**], Hongliang Jiang [a,b,*]

[a] Department of Polymer Science and Engineering, Zhejiang University, Hangzhou 310027, China
[b] MOE Key Laboratory of Macromolecular Synthesis and Functionalization, Zhejiang University, Hangzhou 310027, China

ARTICLE INFO

Article history:
Received 29 October 2013
Received in revised form
23 November 2013
Accepted 25 November 2013
Available online 1 December 2013

Keywords:
Polymeric nanoparticle
Electrospray
Core–shell–corona structure
Size modulation
Drug delivery

ABSTRACT

This study proposed a new strategy based on a coaxial tri-capillary electrospray-template removal process for producing nanosized polylactide-*b*-polyethylene glycol (PLA-PEG) particles with a core–shell structure. Microparticles with core–shell–corona structures were first fabricated by coaxial tri-capillary electrospray, and core–shell nanoparticles less than 200 nm in size were subsequently obtained by removing the PEG template from the core–shell–corona microparticles. The nanoparticle size could be modulated by adjusting the flow rate of corona fluid, and nanoparticles with an average diameter of 106 ± 5 nm were obtained. The nanoparticles displayed excellent dispersion stability in aqueous media and very low cytotoxicity. Paclitaxel was used as a model drug to be incorporated into the core section of the nanoparticles. A drug loading content in the nanoparticles as high as 50.7 ± 1.5 wt% with an encapsulation efficiency of greater than 70% could be achieved by simply increasing the feed rate of the drug solution. Paclitaxel exhibited sustained release from the nanoparticles for more than 40 days. The location of the paclitaxel in the nanoparticles, i.e., in the core or shell layer, did not have a significant effect on its release.

1. Introduction

Drug delivery carriers can be fabricated using several techniques, such as emulsion-solvent evaporation, microfluidic systems, self-assembly and electrospray [1–4]. Of these techniques, the electrospray method has several unique advantages. For example, monodispersed particles can be produced using the cone-jet mode of the electrospray technique, and the particle size can be easily controlled by adjusting the preparation parameters [5–7]. In addition, either hydrophobic or water-soluble drugs can be facilely loaded into electrosprayed particles with high entrapment efficiency [8–12]. Furthermore, core–shell structured particles can be conveniently obtained through coaxial electrospray [4,13]. Compared with the emulsion-solvent evaporation method, which has frequently been used for encapsulating protein drugs into biodegradable microparticles, coaxial electrospray can preserve the structural integrity and bioactivity of protein drugs because there is no direct contact between the proteins and organic solvent during the electrospray process [14,15]. Multidrug encapsulation and multishell encapsulation can also be achieved using tri-capillary coaxial electrospray [10,16,17]. The release profiles of encapsulated drugs can be independently modulated by changing the internal structure and compositions of the particles [11].

Despite the aforementioned advantages, the size of electrosprayed particles was always within micron to submicron range. Many strategies have been developed in an attempt to decrease the particle size. By delicately varying the polymer concentration, feed rate and applied voltage, polymethylsilsesquioxane particles with sizes ranging from 275 to 860 nm were obtained [18]. Drug-loaded polylactide particles with average diameters of approximately 200 nm were produced by reducing the feed rate of the polymer solution and increasing the electrical conductivity of the electrospray solution [12]. By reducing the polymer concentration to as low as 0.01 g/ml and decreasing the fluid flow rate to as slow as 0.036 ml/h, chitosan particles with an average diameter of 124 nm were successfully prepared [19]. However, decreasing the particle size by decreasing either the solution concentration or flow rate would lead to a low particle production capacity. In addition, there have been few reports on the production of polymeric particles with sizes of less than 100 nm. It has been confirmed that the size of drug delivery carriers plays an important role in their in vivo transport behaviors [20]. For example, nanoparticles

* Corresponding author at: Department of Polymer Science and Engineering, Zhejiang University, Zheda Road No. 38, Hangzhou 310027, China.
Tel.: +86 571 87952046.
** Corresponding author at: Department of Polymer Science and Engineering, Zhejiang University, Zheda Road No. 38, Hangzhou 310027, China.
Tel.: +86 571 87952596; fax: +86 571 87952596.
E-mail addresses: caocao2008@zju.edu.cn (L. Cao), m05luojun@zju.edu.cn (J. Luo), tukh@zju.edu.cn (K. Tu), lqwang@zju.edu.cn (L.-Q. Wang), hljiang@zju.edu.cn (H. Jiang).

0927-7765/$ – see front matter © 2013 Elsevier B.V. All rights reserved.
http://dx.doi.org/10.1016/j.colsurfb.2013.11.046

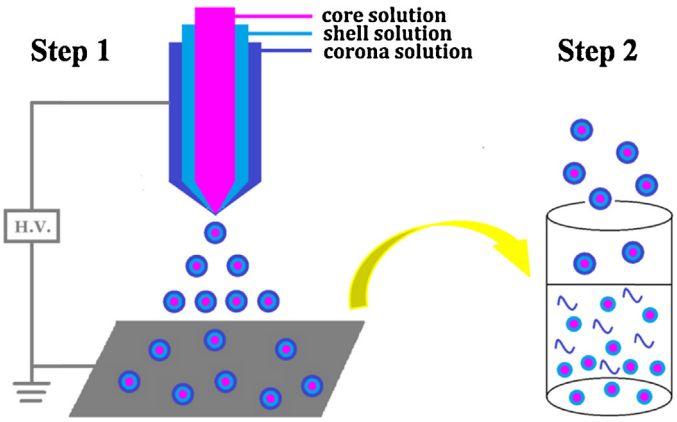

Fig. 1. Schematic diagram of coaxial tri-capillary electrospray-template removal method. Step 1: coaxial tri-capillary electrospray, Step 2: template removal.

presented enhanced colon bioadhesion and increased oral bioavailability compared with microparticles [21,22]. Particles smaller than 500 nm may have the opportunity to escape phagocyte attack in the bloodstream [23]. In addition, particles smaller than 100 nm could be extravasated into tumor tissues through enhanced permeation and retention effects [24]. Thus, it is essential to finely modulate the size of drug delivery carriers to improve therapeutic efficacy, reduce drug dose and minimize unwanted side effects.

In this work, a new strategy was proposed based on a coaxial tri-capillary electrospray-template removal process to control the size of electrosprayed particles. Briefly, microparticles with a core–shell–corona structure were first fabricated through coaxial tri-capillary electrospray. The corona layer was subsequently removed to expose the inner core–shell particles. It was found that core–shell particles with sizes close to 100 nm could be obtained and that the particle size could be conveniently modulated by adjusting flow rate of the corona fluid. The particle properties and cellular uptake were also evaluated. Paclitaxel (PTX) was used as a model drug to be encapsulated into the particles. The drug loading and in vitro release behaviors were investigated. In addition, the effect of the PTX location in the nanoparticles, either in the core or shell section, on its release was investigated.

2. Materials and methods

2.1. Materials

Polyethylene glycol (PEG, Mn = 20,000) was purchased from Sinopharm Chemical Reagent Co. Ltd. Polylactide-*b*-polyethylene glycol (PLA-PEG, PEG10000) was synthesized in our lab, and the number average molecular weight was 46 kDa determined by gel permeation chromatography. PTX was supplied by Hangzhou Haida Pharmaceutical Chemical Co. Ltd. Fluoresceine isothiocyanate (FITC), Nile red and Hochest 33342 were purchased from Sigma–Aldrich. Trifluoroethanol (TFE) was obtained from Weihai Newera Chemical Co. Ltd. RPMI 1640 medium was purchased from Genom biomedical technology Co. Ltd and fetal bovine serum (FBS) was obtained from Zhejiang Tianhang Biomedical Technology Co. Ltd. All other chemicals and solvents were of analytical grade and used as received.

2.2. Fabrication of core–shell–corona microparticles by coaxial tri-capillary electrospray

The schematic diagram of coaxial tri-capillary electrospray system is shown in Fig. 1. The set-up is composed of a tri-capillary spray head, a high-voltage power supply (DW-P503-1ACCC, Tianjin Dongwen High-Voltage Power Supply Co. Ltd, China), three syringe pumps (KDS100, kdScientific, USA) and a collecting plate. The spray head consists of three coaxially arranged stainless needles. The outer diameters (OD) of the three needles are 2.86, 1.70 and 0.80 mm, respectively, and the inner diameters (ID) are 2.06, 1.10 and 0.70 mm, respectively. A foil paper on the platform was used as a collecting plate. The distance between the spray head and the collecting plate was fixed at 16 cm in all experiments. 10% (w/v) PEG solution in TFE was used as corona fluid, 3% (w/v) PLA-PEG solution in chloroform as shell fluid and 3% (w/v) PEG solution in chloroform as core fluid. All three fluids were fed through syringe pumps independently with different feed rate. To visualize the structure of the resultant microparticles, fluorescent dye FITC was contained in core and corona solutions before electrospraying.

2.3. Preparation of nanoparticles from core–shell–corona microparticles

The foil papers for collecting electrosprayed particles were cut into pieces and soaked in deionization water for several hours at room temperature. Afterwards, the suspension was filtered with a low speed quantitative filter paper (retention size 1–3 μm) to remove foil papers and possible aggregates. The filtrate was stored in refrigerator at 4 °C till characterization.

2.4. Characterization of micro- and nanoparticles

The morphologies of the particles were characterized by scanning electron microscope (SEM, Hitachi S-4800, Hitachi, Japan) and transmission electron microscopy (TEM, JEM-1230, JEOL, Japan). The average particle diameters and distributions of microparticles were analyzed with the software Image-Pro Plus (Media Cybernetics, Inc.) ($n = 100$). The particle sizes and Z-potentials of the nanoparticles were determined by nano particle potential analyzer (Malvern ZCEC, Malvern, UK). The structures of the microparticles was observed by laser scanning confocal microscope (LSCM, SP5II, Leica, Germany).

2.5. Dispersion stability of PLA-PEG nanoparticles in water

PLA-PEG nanoparticle solutions prepared according to the procedures described above were stored at 4 °C. The change in the particle size was monitored by nano particle potential analyzer at predetermined time points.

2.6. Cytotoxicity of PLA-PEG nanoparticles

The adenocarcinomic human alveolar basal epithelial cell line A549, which was used for evaluating the cytotoxicity of the PLA-PEG nanoparticles was kindly provided by Professor Guping Tang (Zhejiang University, Hangzhou, China). A549 cells were cultured in RPMI 1640 medium containing 10% FBS, 100 U/ml penicillin and 100 μg/ml streptomycin at 37 °C in 5% CO_2 in a humidified atmosphere. Hydrophobic fluorescent dye Nile red was added into PEG solution (core fluid) before electrospraying in order to visualize the nanoparticles. The particle size and zeta potential of PLA-PEG particles used in cell experiments were 115 ± 10 nm and -8.0 ± 0.5 mV, respectively.

200 μl of the cells were seeded into a 96-well plate (Costar, Corning Corp., NY) at a density of 1×10^4 cells per well. After incubating for 18 h, the culture medium was replaced with nanoparticle solutions, which were serially diluted by serum free culture medium, and incubated for 4 h. Then, the particle solutions were removed and replaced by MTT reagent diluted with serum free culture medium (0.5 mg/ml). After incubating for another

4 h at 37 °C, excess dyes were displaced with 150 μl dimethylsulfoxide per well. Microplate reader (Multiskan MK3, Thermo Scientific, USA) was used to measure the adsorption value at a wavelength of 570 nm. RPMI 1640 and polyethylenimine (25 kDa, 10 mg/ml) were used as negative and positive controls, respectively. The cytotoxicity was expressed as a percentage of the control.

2.7. Cellular uptake of PLA-PEG nanoparticles

A549 cells were seeded in a glass bottom cell culture dish (Costar, Corning Corp., NY) at a density of 20×10^4 cells per well and incubated overnight. Cells were washed with phosphate buffer saline (PBS) and then treated with 100 μg/ml of PLA-PEG nanoparticle solution which was diluted with culture medium containing 2% FBS for 12 h at 37 °C in 5% CO_2 in a humidified atmosphere. To observe cellular uptake of the particles, treated cells were washed with PBS three times, stained with Hochest 33342 (nucleus stain) and imaged with LSCM.

2.8. Drug loading and in vitro release

PTX was selected as a model drug, which was widely used in treatments of lung cancer as well as breast and ovarian cancers. 10% (w/v) PTX dissolved in chloroform was used as core fluid, 3% (w/v) PLA-PEG as the shell fluid and 10% (w/v) PEG as corona fluid. The flow rates of shell and corona fluids were fixed at 0.5 and 0.8 ml/h, respectively. The flow rate of drug solution was adjusted from 0.2 to 0.3 ml/h to achieve different drug loading contents in the nanoparticles. To investigate the effect of microenvironment around PTX on drug release profile, PTX was incorporated into the shell layer of the nanoparticles by using PLA-PEG solution containing 5.6% (w/v) PTX as shell fluid, 3% (w/v) PEG as core fluid and 10% (w/v) PEG as the corona fluid. To achieve particles with similar drug loading content with particles prepared through 0.2 ml/h PTX described above, the flow rates of core, shell and corona fluid were fixed at 0.2, 0.5 and 0.8 ml/h, respectively. The drug loading content and entrapment efficiency were determined by high-performance liquid chromatography analysis (HPLC). A C-18 column (4.6 mm × 250 mm, Welch Materials Inc., China) was used. The mobile phase was consisted of a mixture of methanol, acetonitrile and water (23:36:41, v/v/v) and delivered flow rate was 1 ml/min according to Chinese Pharmacopeia 2010. The detector wavelength for the HPLC detection was set at 227 nm. Drug-loaded particles collected from foil paper were first dissolved in dichloromethane, then added with methanol to dissolve PTX and finally vacuum dried [25]. A standard plot for PTX was prepared in either methanol or PBS containing 0.5% (w/v) Tween 80 for determining drug loading content and in vitro release respectively. Drug loading content was defined as the amount of drug (in mg) present in 100 mg of nanoparticles. Drug entrapment efficiency (%) was expressed as the percent of added drug that was entrapped in nanoparticles.

The drug release profiles were determined in PBS containing 0.5% (w/v) Tween 80. The particles fabricated by coaxial tri-capillary electrosray were collected from foil paper and put in a dialysis tube (Molecular weight cut off = 3500) containing 2 ml release medium. The dialysis tubes were then soaked in 30 ml release medium and incubated at 37 °C with continuous shaking. At the scheduled time interval, all release medium was withdrawn and 30 ml of fresh release medium was added. The PTX concentration in the release medium was determined by HPLC described before in triplicate.

2.9. Statistical analysis

All data were displayed as mean ± SD in the study. Statistical analysis was conducted using Student's *t*-test and statistical significance was set at $p < 0.05$.

3. Results and discussion

3.1. Fabrication of PLA-PEG nanoparticles through the coaxial tri-capillary electrospray-template removal method

In this study, a coaxial tri-capillary electrospray-template removal method was developed to prepare nanosized drug carriers. Briefly, core–shell–corona microparticles were first fabricated by coaxial tri-capillary electrospray; subsequently, the water-soluble corona template was removed by water treatment to obtain nanosized particles. A schematic diagram of the fabrication process is shown in Fig. 1. PEG was selected as the corona template material because of its water solubility and biocompatibility. The amphiphilic diblock copolymer PLA-PEG was used as a shell material due to its excellent biodegradability, biocompatibility and stealth surface characteristics.

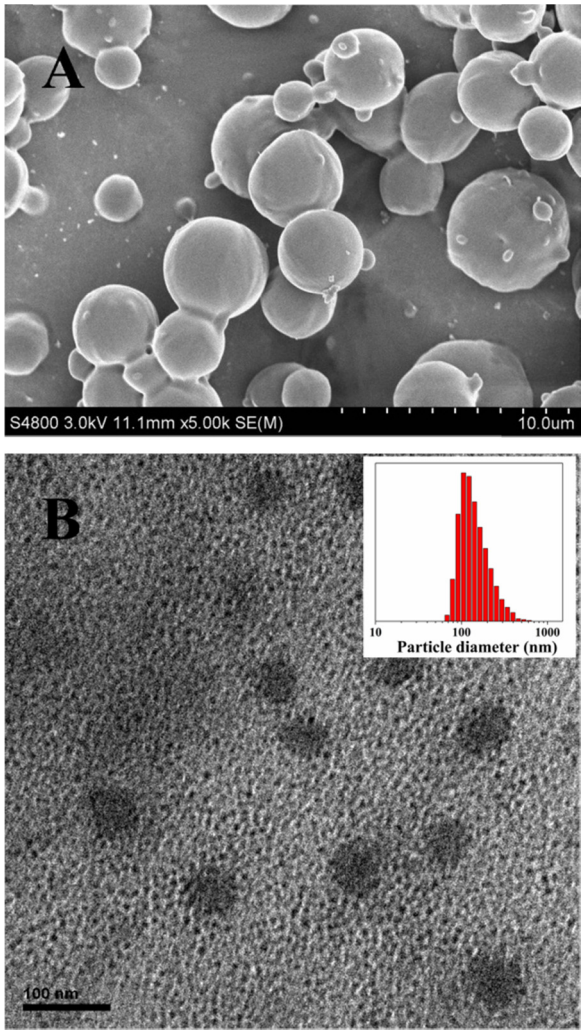

Fig. 2. (A) SEM image of PEG/PLA-PEG/PEG microparticles. Flow rates of core, shell and corona fluids were set at 0.3, 0.5 and 1.0 ml/h, respectively. (B) TEM image of the nanoparticles prepared by removing PEG template from core–shell–corona microparticles. Scale bar = 100 nm. The inset in the upper right corner of (B) shows size distribution of the nanoparticles determined by nano particle potential analyzer.

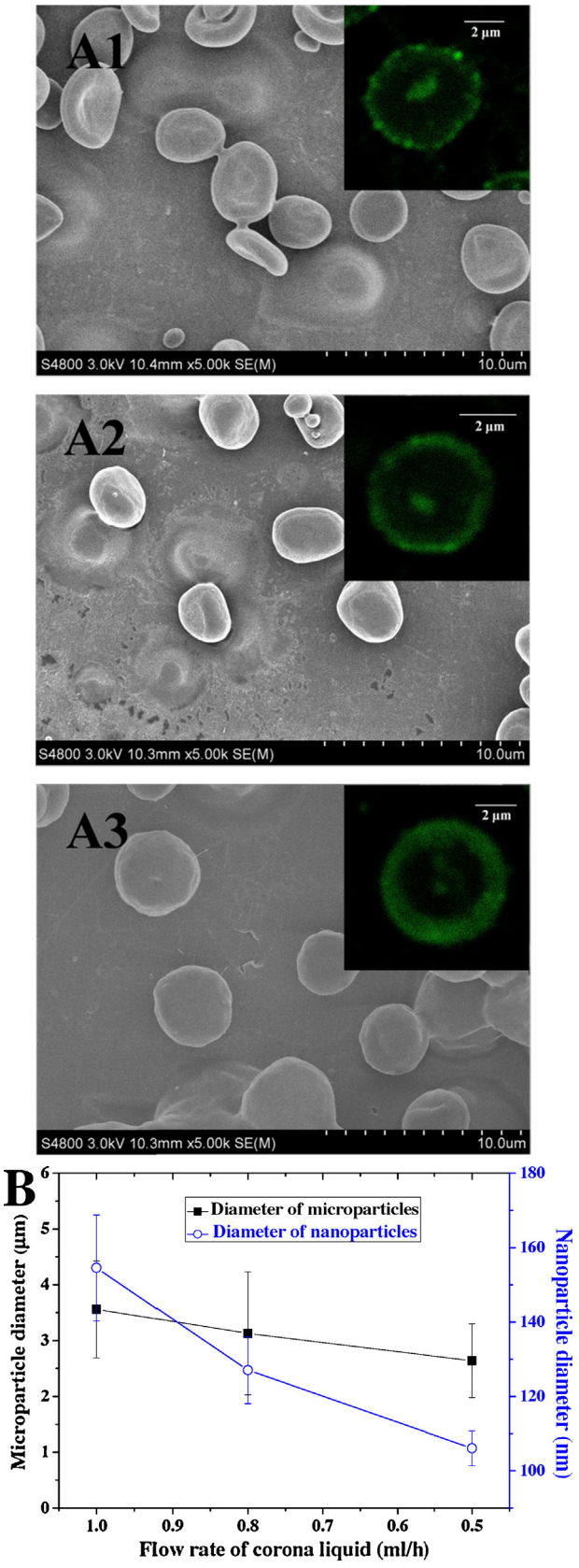

The morphologies of the microparticles fabricated by coaxial tri-capillary electrospray are shown in Fig. 2A. Spherical microparticles with smooth surfaces were obtained, and the average size diameter was 3.56 ± 0.87 μm when the flow rates of the core, shell and corona fluids were 0.3, 0.5 and 1.0 ml/h, respectively. Submicron particles and even smaller fragments could be observed, which might be fission products from solvent evaporation. The droplet ejected from the spray head gradually shrank before traveling to the collecting plate due to solvent evaporation. This resulted in the enrichment of the surface charges. When the charges on the droplet reached the Rayleigh charge limit, which constitutes a critical condition when the electric force overcomes the liquid surface tension, Rayleigh fission occurred [26,27]. The subsequent removal of the PEG corona layer yielded PLA-PEG nanoparticles with an average hydrate diameter of 155 ± 14 nm (Fig. 2B inset). TEM image also revealed a significant decrease in the particle size after template removal (Fig. 2B). It was also observed that the particles remained spherical after removing the PEG template. All the above results confirmed the feasibility of the proposed strategy based on a coaxial tri-capillary electrospray-template removal method for fabricating nanosized particles.

To visualize the internal structure of the electrosprayed microparticles, core and corona layers were all labeled with FITC. To enhance the contrast between the different layers, the flow rate of the shell fluid was increased to 1.0 ml/h to increase the thickness of the shell layer. The flow rate of the core fluid was fixed at 0.2 ml/h and that of the corona fluid was varied from 0.1 to 0.5 ml/h. LSCM images revealed that the resulting microparticles displayed a distinct core–shell–corona structure (Fig. 3A1, A2 and A3 insets). Flat-shaped microparticles were obtained when the flow rate of the corona fluid was 0.1 ml/h (Fig. 3A1). It was also observed in the LSCM image (Fig. 3A1 inset) that the corona layer was discontinuous, indicating that the flow rate of the corona fluid was too slow to form an integrated layer around the inner shell section. By increasing the flow rate of the corona fluid to 0.5 ml/h, the microparticles were transformed into spheres with a continuous corona layer (Fig. 3A3). At a low corona fluid feed rate, the corona fluid (PEG solution in TFE) could not completely wrap the shell fluid (PLA-PEG solution in chloroform), resulting in the exposure of chloroform to air. The rapid evaporation of chloroform from the shell fluid resulted in the formation of a skin layer around the droplets, limiting the gradual shrinkage of the droplets. Further evaporation of the solvents in the droplets led to collapse of the droplets and the formation of flat microparticles. The relatively slow evaporation of TFE due to its higher boiling point might prevent the formation of the skin layer and facilitate the generation of spherical microparticles with a high corona fluid feed rate. The thickness of the corona layer in the microparticles was also observed to increase as the feed rate of the corona fluid increased. The above results demonstrated that the layer thickness of the particles could be modulated by varying the flow rate of the corona fluid [10], which provides a convenient method for manipulating the sizes of the inner core–shell particles.

Fig. 3B shows the effect of the corona fluid feed rate on the sizes of the microspheres before and after water treatment. The flow rates of the core and shell fluids were fixed at 0.3 and 0.5 ml/h. As the

Fig. 3. (A) The effect of corona fluid flow rate on the structure of microparticles. (A1, A2 and A3) SEM images of microparticles. The flow rates of the core and shell fluids were fixed at 0.2 and 1.0 ml/h, while the corona fluid flow rates were (A1) 0.1, (A2) 0.2 and (A3) 0.5 ml/h. The insets in the upper right corner of SEM images were corresponding LSCM images of microparticles. Core and corona layers were labeled by FITC. (B) The effect of corona fluid flow rate on the size of the microparticles before and after water treatment. The flow rates of the core and shell fluids were fixed at 0.3 and 0.5 ml/h, while the corona fluid flow rates were decreased from 1.0 to 0.5 ml/h.

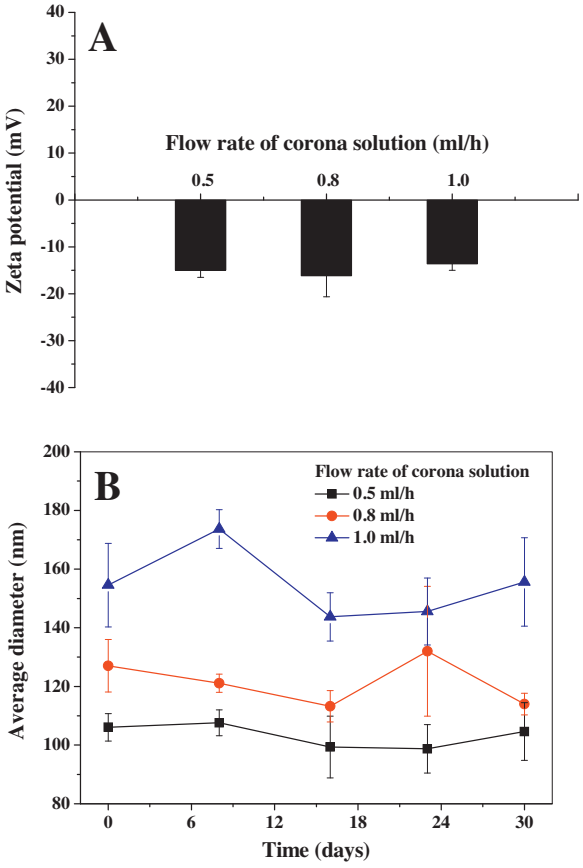

Fig. 4. (A) Zeta potentials of PLA-PEG nanoparticles in water; (B) dispersion stability of PLA-PEG nanoparticles in water. The flow rates of the core and shell fluids were fixed at 0.3 and 0.5 ml/h, respectively.

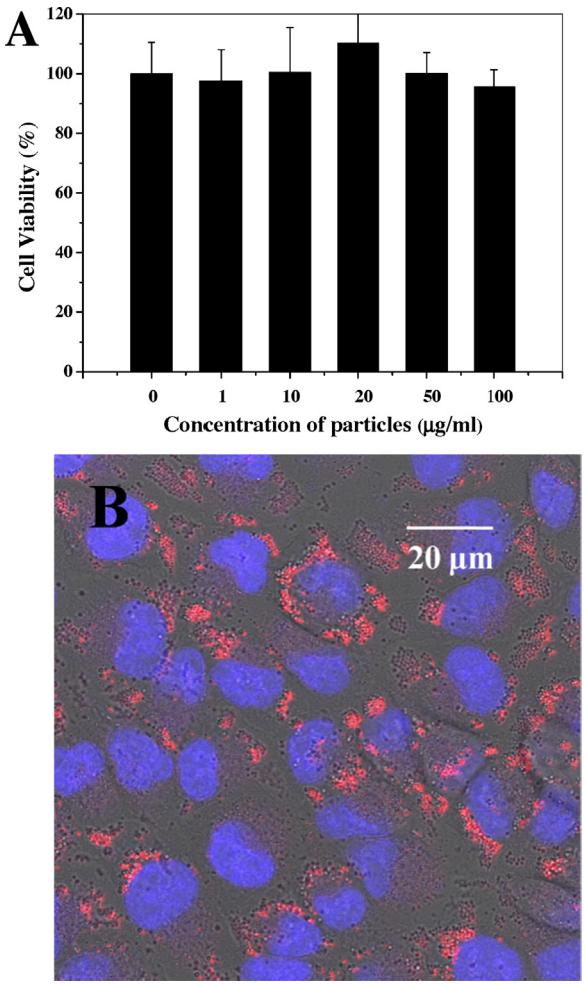

Fig. 5. (A) Viability of the cells exposed to PLA-PEG nanoparticles ($n = 3$, * $p < 0.05$). (B) Merged LSCM image of A549 cells after incubated with PLA-PEG nanoparticles for 12 h. The nanoparticle concentration was 100 μg/ml. Fluorescence image shows cell nucleus (blue) and nanoparticles (red). Scale bar = 20 μm. (For interpretation of the references to colour in this figure legend, the reader is referred to the web version of this article.)

flow rate of the corona fluid was decreased from 1.0 to 0.5 ml/h, the average diameter of the microparticles decreased from 3.56 ± 0.87 to 2.64 ± 0.66 μm, respectively, which resulted in the decrease of the corresponding nanoparticles from 155 ± 14 to 106 ± 5 nm.

3.2. Properties of PLA-PEG nanoparticles

The surfaces of all nanoparticle prepared at different corona fluid feed rates are negatively charged with a zeta potential of approximately −15 mV (Fig. 4A). This negative surface charge can be due to the presence of carboxyl groups at the surfaces of the nanoparticles [28]. In addition, the nanoparticles displayed excellent dispersion stability. The diameter of the nanoparticles remained almost unchanged during the evaluation period (30 days) at 4 °C (Fig. 4B). The presence of negative charges and PEG segments both contributed to the observed dispersion stability of the nanoparticles. Similar results were also reported for PLA-PEG nanoparticles prepared using other techniques [29,30].

The cytotoxicity of PLA-PEG nanoparticles was evaluated using an MTT assay. The cell viability approached 100% even when the nanoparticle concentration reached 100 μg/ml (Fig. 5A), suggesting high biocompatibility of the nanoparticles. To monitor the cellular uptake of the nanoparticles, the nanoparticles were fluorescently labeled with Nile red. It could be observed that the nanoparticles could be uptaken by A549 cells and enriched around the nucleus (Fig. 5B); however, there were no particles penetrating through the nuclear envelope and residing in the nucleus.

3.3. Drug loading and in vitro release

Ideal drug delivery carriers should not only have an appropriate size for overcoming different biological barriers but also have the capacity to load diverse drug payloads with reasonable loading contents and high loading efficiencies. It was reported that the electrospray technique can always achieve high drug loading efficiencies compared with other encapsulation techniques, such as emulsion-solvent evaporation [9,11,31]. However, there are few reports concerning the drug loading capacity of electrospray. In this study, the drug loading content was modulated by changing the flow rate of the core drug solution. It was found that the drug loading content in PLA-PEG nanoparticles increased from 44.5 ± 0.9% to 50.7 ± 1.5% when the flow rate of the PTX solution was increased from 0.2 to 0.3 ml/h without compromising the stability of the electrospray process or the drug entrapment efficiency (>70%) (Table 1). Compared with other techniques such as self-assembly and emulsion-solvent evaporation, the drug loss during the electrospray process was insignificant. Achieving a high drug loading content in electrosprayed particles might be limited by the possibility of the high drug solution feed rate destabilizing the electrospray process. In this study, the electrospray process became unstable when the flow rate of the drug fluid was greater than 0.8 ml/h, corresponding to a loading content of PTX of 84%. Drug release profiles

Table 1
Drug loading contents and entrapment efficiencies of various particles.

Composition	Flow rate (ml/h)	Loading content (%)	Entrapment efficiency (%)
PTX/PLA-PEG/PEG[a]	0.2/0.5/0.8[b]	44.5 ± 0.9	77.9 ± 1.6
PTX/PLA-PEG/PEG	0.3/0.5/0.8	50.7 ± 1.5	76.2 ± 2.3
PEG/PTX +PLA-PEG/PEG[c]	0.2/0.5/0.8	41.1 ± 1.0	72.0 ± 1.7

[a] Materials of core–shell–corona.
[b] Flow rate of core–shell–corona.
[c] PTX was encapsulated into shell layer.

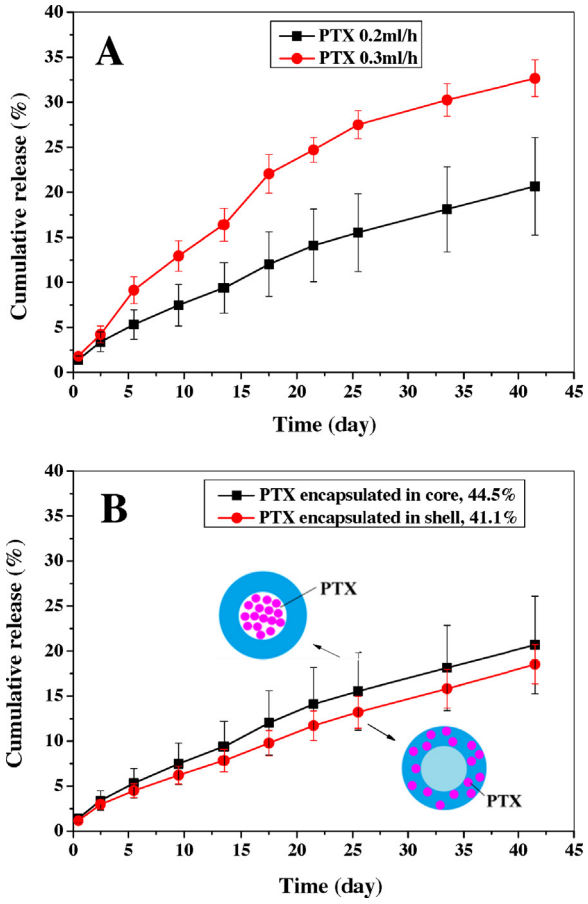

Fig. 6. (A) Effect of drug loading content on PTX release. (B) Effect of drug location on PTX release. The insets of (B) were schematic diagrams of nanoparticles encapsulating drugs in core or shell layer.

from the nanoparticles are shown in Fig. 6. Sustained release of PTX could be achieved with a near zero order for more than 40 days. It was reported that the release of PTX from PLGA nanoparticles produced by emulsion solvent evaporation could last more than 35 days [32]. In contrast, the release of PTX from PLA-PEG micelles was very rapid, within almost one day [33,34]. The nanoparticles with higher PTX loadings showed faster drug release (Fig. 6A). To investigate the effect of the microenvironment around PTX on the drug release behavior, particles with PTX incorporated into the PLA-PEG layer were prepared. The drug loading percent and encapsulation efficiency were 41.1 ± 1.0% and 72.0 ± 1.7%, respectively (Table 1). The location of PTX in the nanoparticles has no significant effect on its release (Fig. 6B).

4. Conclusions

In summary, core–shell PLA-PEG nanoparticles approximately 100 nm in size were successfully produced using a coaxial tri-capillary electrospray-template removal method. The particle size could be modulated by adjusting the flow rate of the corona fluid. The nanoparticles had good dispersion stability in water and very low cytotoxicity. In addition, PLA-PEG nanoparticles could be enriched around the nucleus of A549 cells but not in the nucleus. PTX could be incorporated into nanoparticles with both a high drug loading content and entrapment efficiency. A sustained release of PTX from the nanoparticles could be achieved for more than 40 days. The proposed strategy for fabricating nanosized core–shell particles is promising for nanomedicine applications.

Acknowledgements

The work was financially supported by the National Science Foundation of China (21274124, 21174125, 21074112), and National Basic Research Program of China (2009CB930104).

References

[1] R. Manchanda, A. Fernandez-Fernandez, A. Nagesetti, A.J. McGoron, Preparation and characterization of a polymeric (PLGA) nanoparticulate drug delivery system with simultaneous incorporation of chemotherapeutic and thermo-optical agents, Colloids Surf. B: Biointerfaces 75 (2010) 260–267.
[2] H.J. Oh, S.H. Kim, J.Y. Baek, G.H. Seong, S.H. Lee, Hydrodynamic microencapsulation of aqueous fluids and cells via 'on the fly' photopolymerization, J. Micromech. Microeng. 16 (2006) 285–291.
[3] C. Zhang, Q.N. Ping, H.J. Zhang, Self-assembly and characterization of paclitaxel-loaded N-octyl-O-sulfate chitosan micellar system, Colloids Surf. B: Biointerfaces 39 (2004) 69–75.
[4] I.G. Loscertales, A. Barrero, I. Guerrero, R. Cortijo, M. Marquez, A.M. Ganan-Calvo, Micro/nano encapsulation via electrified coaxial liquid jets, Science 295 (2002) 1695–1698.
[5] K.M. Yun, A.B. Suryamas, C. Hirakawa, F. Iskandar, K. Okuyama, A new physical route to produce monodispersed microsphere nanoparticle–polymer composites, Langmuir 25 (2009) 11038–11042.
[6] H. Widiyandari, C.J. Hogan, K.M. Yun Jr., F. Iskandar, P. Biswas, K. Okuyama, Production of narrow-size-distribution polymer–pigment–nanoparticle composites via electrohydrodynamic atomization, Macromol. Mater. Eng. 292 (2007) 495–502.
[7] L. Ding, T. Lee, C.H. Wang, Fabrication of monodispersed taxol-loaded particles using electrohydrodynamic atomization, J. Control. Release 102 (2005) 395–413.
[8] H. Nie, Z. Dong, D.Y. Arifin, Y. Hu, C.-H. Wang, Core/shell microspheres via coaxial electrohydrodynamic atomization for sequential and parallel release of drugs, J. Biomed. Mater. Res. A 95A (2010) 709–716.
[9] Y. Wang, X. Yang, W. Liu, F. Zhang, Q. Cai, X. Deng, Controlled release behaviour of protein-loaded microparticles prepared via coaxial or emulsion electrospray, J. Microencapsul. 30 (2013) 490–497.
[10] W. Kim, S.S. Kim, Synthesis of biodegradable triple-layered capsules using a triaxial electrospray method, Polymer 52 (2011) 3325–3336.
[11] Y.-H. Lee, M.-Y. Bai, D.-R. Chen, Multidrug encapsulation by coaxial tri-capillary electrospray, Colloids Surf. B: Biointerfaces 82 (2011) 104–110.
[12] H. Valo, L. Peltonen, S. Vehvilainen, M. Karjalainen, R. Kostiainen, T. Laaksonen, J. Hirvonen, Electrospray encapsulation of hydrophilic and hydrophobic drugs in poly(L-lactic acid) nanoparticles, Small 5 (2009) 1791–1798.
[13] S. Zhang, K. Kawakami, M. Yamamoto, Y. Masaoka, M. Kataoka, S. Yamashita, S. Sakuma, Coaxial electrospray formulations for improving oral absorption of a poorly water-soluble drug, Mol. Pharm. 8 (2011) 807–813.
[14] J. Xie, W.J. Ng, L.Y. Lee, C.-H. Wang, Encapsulation of protein drugs in biodegradable microparticles by co-axial electrospray, J. Colloid Interface Sci. 317 (2008) 469–476.
[15] H.L. Jiang, Y.Q. Hu, Y. Li, P.C. Zhao, K.J. Zhu, W.L. Chen, A facile technique to prepare biodegradable coaxial electrospun nanofibers for controlled release of bioactive agents, J. Control. Release 108 (2005) 237–243.
[16] Z. Ahmad, H.B. Zhang, U. Farook, M. Edirisinghe, E. Stride, P. Colombo, Generation of multilayered structures for biomedical applications using a novel tri-needle coaxial device and electrohydrodynamic flow, J. R. Soc. Interface 5 (2008) 1255–1261.

[17] W. Kim, S.S. Kim, Multishell encapsulation using a triple coaxial electrospray system, Anal. Chem. 82 (2010) 4644–4647.
[18] M.-W. Chang, E. Stride, M. Edirisinghe, A new method for the preparation of monoporous hollow microspheres, Langmuir 26 (2010) 5115–5121.
[19] S. Zhang, K. Kawakami, One-step preparation of chitosan solid nanoparticles by electrospray deposition, Int. J. Pharm. 397 (2010) 211–217.
[20] S. Mitragotri, J. Lahann, Physical approaches to biomaterial design, Nat. Mater. 8 (2009) 15–23.
[21] A. Lamprecht, U. Schafer, C.M. Lehr, Size-dependent bioadhesion of micro- and nanoparticulate carriers to the inflamed colonic mucosa, Pharm. Res. 18 (2001) 788–793.
[22] K. Sigfridsson, A. Nordmark, S. Theilig, A. Lindahl, A formulation comparison between micro- and nanosuspensions: the importance of particle size for absorption of a model compound, following repeated oral administration to rats during early development, Drug Dev. Ind. Pharm. 37 (2011) 185–192.
[23] R.C. May, L.M. Machesky, Phagocytosis and the actin cytoskeleton, J. Cell Sci. 114 (2001) 1061–1077.
[24] Y. Matsumura, H. Maeda, A new concept for macromolecular therapeutics in cancer-chemotherapy – mechanism of tumoritropic accumulation of proteins and the antitumor agent smancs, Cancer Res. 46 (1986) 6387–6392.
[25] C. Vilos, F.A. Morales, P.A. Solar, N.S. Herrera, F.D. Gonzalez-Nilo, D.A. Aguayo, H.L. Mendoza, J. Comer, M.L. Bravo, P.A. Gonzalez, S. Kato, M.A. Cuello, C. Alonso, E.J. Bravo, E.I. Bustamante, G.I. Owen, L.A. Velasquez, Paclitaxel-PHBV nanoparticles and their toxicity to endometrial and primary ovarian cancer cells, Biomaterials 34 (2013) 4098–4108.
[26] H. Oh, S. Kim, Synthesis of ceria nanoparticles by flame electrospray pyrolysis, J. Aerosol Sci. 38 (2007) 1185–1196.
[27] J.F. delaMora, On the outcome of the Coulombic fission of a charged isolated drop, J. Colloid Interface Sci. 178 (1996) 209–218.
[28] H.S. Yoo, K.H. Lee, J.E. Oh, T.G. Park, In vitro and in vivo anti-tumor activities of nanoparticles based on doxorubicin-PLGA conjugates, J. Control. Release 68 (2000) 419–431.
[29] X. Shan, C. Liu, Y. Yuan, F. Xu, X. Tao, Y. Sheng, H. Zhou, In vitro macrophage uptake and in vivo biodistribution of long-circulation nanoparticles with poly(ethylene-glycol)-modified PLA (BAB type) triblock copolymer, Colloids Surf. B: Biointerfaces 72 (2009) 303–311.
[30] Y. Sheng, Y. Yuan, C. Liu, X. Tao, X. Shan, F. Xu, In vitro macrophage uptake and in vivo biodistribution of PLA-PEG nanoparticles loaded with hemoglobin as blood substitutes: effect of PEG content, J. Mater. Sci. Mater. Med. 20 (2009) 1881–1891.
[31] M.J. Cozar-Bernal, M.A. Holgado, J.L. Arias, I. Munoz-Rubio, L. Martin-Banderas, J. Alvarez-Fuentes, M. Fernandez-Arevalo, Insulin-loaded PLGA microparticles: flow focusing versus double emulsion/solvent evaporation, J. Microencapsul. 28 (2011) 430–441.
[32] M.D. Chavanpatil, Y. Patil, J. Panyam, Susceptibility of nanoparticle-encapsulated paclitaxel to P-glycoprotein-mediated drug efflux, Int. J. Pharm. 320 (2006) 150–156.
[33] H.-C. Shin, A.W.G. Alani, H. Cho, Y. Bae, J.M. Kolesar, G.S. Kwon, A 3-in-1 polymeric micelle nanocontainer for poorly water-soluble drugs, Mol. Pharm. 8 (2011) 1257–1265.
[34] U. Katragadda, Q. Teng, B.M. Rayaprolu, T. Chandran, C. Tan, Multi-drug delivery to tumor cells via micellar nanocarriers, Int. J. Pharm. 419 (2011) 281–286.